

UNIVERSITY OF SOUTHERN CALIFORNIA
DEPARTMENT OF CIVIL ENGINEERING

DEPENDENCE OF THE FOURIER AMPLITUDE SPECTRA OF
STRONG MOTION ACCELERATION ON THE DEPTH OF SEDIMENTARY DEPOSITS

by

Mihailo D. Trifunac and Vincent W. Lee

Report No. CE 78-14

A Report on the Research Conducted Under a
Contract from the U.S. Nuclear Regulatory Commission

Los Angeles, California

December, 1978

ABSTRACT

In this report, we present an improvement in empirical scaling of Fourier spectrum amplitudes of strong motion earthquake accelerations by introducing the frequency dependent effects of local geologic conditions, characterized by the depth of sediments beneath the recording station. Equations presented here lead to smaller spread of data about the empirical models than previous related empirical scaling of Fourier spectrum amplitudes (Trifunac, 1976a,b; 1978a,b). Simplified statistical tests on the significance of chosen parameters and of the regression equations show significant increase in spectral amplitudes with the depth of sediments for periods longer than about 1 second. For high frequencies, this trend is reversed, but small. It is concluded therefore that the local geologic site conditions play a prominent role in shaping the expected amplitudes of Fourier spectra of strong motion acceleration.

INTRODUCTION

Several recent studies on the influence of the recording site conditions on the amplitudes of strong ground motion have shown that these appear to have a significant frequency dependent effect. However, the incomplete data base and different interpretation of what should be considered to represent the recording site conditions have resulted in a variety of scaling models, none of which, so far, may have achieved the needed precision and optimum choice of scaling parameters. In 1974, Seed, Ugas and Lysmer (Seed, et. al., 1974) presented a method for description of the recording site conditions. Their approach consists of classifying the local soils into four groups: (i) rock, (ii) stiff soils, (iii) deep cohesionless soils, and (iv) soft to medium clay and sand. By analyzing separately recordings of strong shaking obtained under these four conditions, they show the resulting trends in the spectral amplitudes to be sensitive to this type of classification. In 1975, Trifunac and Brady presented a different method for site classification which emphasized geological rather than soil mechanics aspects of the earth materials beneath the recording stations. They proposed to classify all recording site conditions into soft (sedimentary deposits, alluvium) or hard (sound basement rock) sites depending on the geology beneath and surrounding the recording. This classification essentially represents a discretization of information on site geology on a scale measured in kilometers. In contrast, the site classification of Seed, et. al. (1974) focuses on the site classification measured on the scale of tens of meters.

In spite of the significant differences in the dimensions involved in these two classification methods, the end results in comparing the observed trends of spectral amplitudes (Trifunac, 1977; 1978a) are similar. Further analyses of the data shows that this similarity results from the fact that for most of the "soft" sites of Trifunac and Brady (1975), the classification of Seed, et. al. (1974) assigns the category of stiff soils, deep cohesionless soils or the soft to medium clay.

The weakness of both above classification methods is that the geometric characteristics of local site conditions are overlooked. While the classification of Seed, et. al. (1974) does reflect some differences in soil depth, the classification of Trifunac and Brady (1975) formally ignores the depth and the horizontal extent of sedimentary deposits and of alluvium. Since the strong ground motion is a wave propagation phenomenon, in which the size of discontinuity relative to the incident wave length must play a prominent role (e.g., Wong and Trifunac, 1977) it is clear that a better and more detailed recording site description would include at least some of its geometric properties. Of course, it must be remembered that in many instances, little or no data may be available for any detailed site classification. Under such circumstances and depending on the frequencies involved in a particular problem, the above method using geologic site classification seems to be appropriate.

The aim of this analysis is to examine whether the accuracy, with which Fourier amplitude spectra of ground acceleration can be empirically estimated, can be improved by introducing a measure of the depth of sedimentary deposits as a site characteristic. There is no doubt that for

a precise site characterization, only one site dimension is far from sufficient. In general, however, wave velocities, material rigidity and density increase with depth. While these increases are often irregular functions of vertical distance, significant increases from sediments to sound igneous rock and across different crustal discontinuities are well documented (e.g., Richter, 1958). Thus, from the wave propagation viewpoint, impedance jumps across these discontinuities must play an important role in governing reflection and refraction of body waves and the interference of guided rays for surface waves. The depth to these discontinuities has also been shown to influence the duration of strong ground motion (Westermo and Trifunac, 1978; 1979). Motivated by these reasons, we choose to introduce the thickness of sedimentary deposits (depth, h) as one scaling parameter for empirical estimation of spectral amplitudes.

The estimates of the depth of sedimentary deposits for past recordings range from 0 km to over 6 km (Westermo and Trifunac, 1978). If viewed in the wave length scale, it is seen that these depths correspond to wave lengths (frequencies) which are representative of strong ground motion. Other characteristics of the data base employed in this study have been discussed previously in connection with similar regression analyses involving Fourier amplitude spectra (Trifunac, 1976a; 1978b) and will not be repeated here. For comparative analyses dealing with the site classification which neglects the depth of sediments, Trifunac and Brady (1975) discuss how this classification was defined as well as the final assignment of site classification to 186 free-field strong motion records.

SCALING OF FOURIER AMPLITUDE SPECTRA IN TERMS OF M, R, h, AND v

Trifunac (1976a) suggested that the Fourier amplitude spectra (FS) of strong motion acceleration can be scaled in terms of the definition of the earthquake magnitude scale and the "correction" function which incorporates the effects of: (1) distribution of observations with respect to the assumed empirical model, (2) geologic site conditions, (3) horizontal versus vertical ground motion differences, and (4) the frequency dependent attenuation effects. Since the aim of this analysis is to further refine the original scaling equation of Trifunac (1976a) by providing a more continuous dependence of spectral amplitudes on the "size" of geologic discontinuities, we replace the scaling parameter s (Trifunac, 1976a; $s=0$ for alluvium, $s=2$ for basement rock and $s=1$ for intermediate sites) by h , which now represents the depth of sediments beneath the recording station. The new scaling equation then becomes

$$\log_{10}[FS(T)] = M + \log_{10}A_0(R) - b(T)M - c(T) - d(T)h - e(T)v - f(T)M^2 - g(T)R, \quad (1)$$

where $FS(T)$ is the Fourier amplitude spectrum at period of vibration, T , M is the published earthquake magnitude, h is the depth of sediments in kilometers, $v=0$ represents horizontal and $v=1$ vertical ground motion, and R is epicentral distance in kilometers. $\log_{10}A_0(R)$ stands for the amplitude attenuation function (Richter, 1958) empirically determined for southern California and representative of wave frequencies centered near the middle of the frequency band for the data used in this study (0.1 Hz to 25 Hz). Functions $b(T)$, $c(T)$, ..., and $g(T)$ are estimated by regression analysis at 91 periods T between 0.04 sec and 15 sec.

To minimize the possible bias in the model equation (1) which could result from uneven distribution of data among the magnitude ratings and from excessive contribution to the data base from the small number of well recorded earthquakes, in this analysis, the data selection prior to the regression analysis was carried out as proposed by Trifunac (1978a,b). Furthermore, to facilitate the comparison of the results in this analysis with the results of previous regression analyses (Trifunac, 1976a,b; 1978a,b), identical computer programs were employed to screen the data for this work as for the original analyses based on the site classifications. Thus, identical accelerograms were chosen for the regression of equation (1) as for all corresponding previous studies (Trifunac, 1976a,b; 1978a,b).

There is no physical basis to assume that the $\log_{10} F_S(T)$ should be a linear function of the depth of sediments, h . The overall trend of spectral amplitudes to increase in the long period range for alluvium sites versus rock sites and the opposite trend for the highest frequency amplitudes was known from the previous analyses, but the functional form of these trends is as yet completely unknown. Thus, before choosing the final form for equation (1) studies were made to find whether there is a significant dependence of spectral amplitudes on powers of h higher than 1. The data available so far, and the least squares method of determining the scaling functions $b(T)$, $c(T)$, ..., suggested that the coefficient functions multiplying h^2 , h^3 and higher powers of h are undistinguishable from zero at the 95% confidence level. This leads to the selection of the final regression model (1) which involves only the linear term in h , $d(T)h$.

Let $\hat{b}(T)$, $\hat{c}(T)$, ..., and $\hat{g}(T)$ represent the least squares estimates for $b(T)$, $c(T)$, ..., and $g(T)$. $\hat{FS}(T)$ in

$$\log_{10}[\hat{FS}(T)] = M + \log_{10}A_0(R) - \hat{b}(T)M - \hat{c}(T) - \hat{d}(T)h - \hat{e}(T)v - \hat{f}(T)M^2 - \hat{g}(T)R \quad (2)$$

then represents the least squares estimate of the Fourier amplitude spectrum at period T . The residuals

$$\epsilon(T) = \log_{10}[FS(T)] - \log_{10}[\hat{FS}(T)] \quad , \quad (3)$$

where $FS(T)$ is the Fourier amplitude spectrum computed from recorded accelerograms, describes the distribution of observed $FS(T)$ about the estimated $\hat{FS}(T)$. In this work, we assume that $\epsilon(T)$ can be described by a normal distribution function with mean $\mu(T)$ and standard deviation $\sigma(T)$ as follows:

$$p(\epsilon, T) = \frac{1}{\sigma(T) \sqrt{2\pi}} \int_{-\infty}^{\epsilon(T)} \exp \left[-\frac{1}{2} \left(\frac{x - \mu(T)}{\sigma(T)} \right)^2 \right] dx \quad . \quad (4)$$

In (4), $p(\epsilon, T)$ represents the probability that $\log_{10}[FS(T)] - \log_{10}[\hat{FS}(T)] \leq \epsilon(T)$.

Figure 1 shows $\hat{b}(T)$, $\hat{c}(T)$... and $\hat{g}(T)$ (full lines) and the estimates of their 95% confidence intervals (Westermo and Trifunac, 1978). Table Ia presents the coefficients $b(T)$ through $g(T)$ in (1) and $\mu(T)$ and $\sigma(T)$ in (4) at eleven selected periods. Table Ib shows the amplitudes of $\log_{10}A_0(R)$ versus epicentral distance (Trifunac, 1976a).

The probability $p^*(\epsilon, T)$ that $\epsilon(T)$ will not be exceeded can be evaluated at a fixed T by finding the fraction of residuals $\epsilon(T)$ (from the total sample of 546) which are smaller than a chosen value. For $p^*(\epsilon, T)$ calculated at 91 periods, $\epsilon(T)$ corresponding to $p^* = 0.1, 0.2, \dots, 0.8$ and

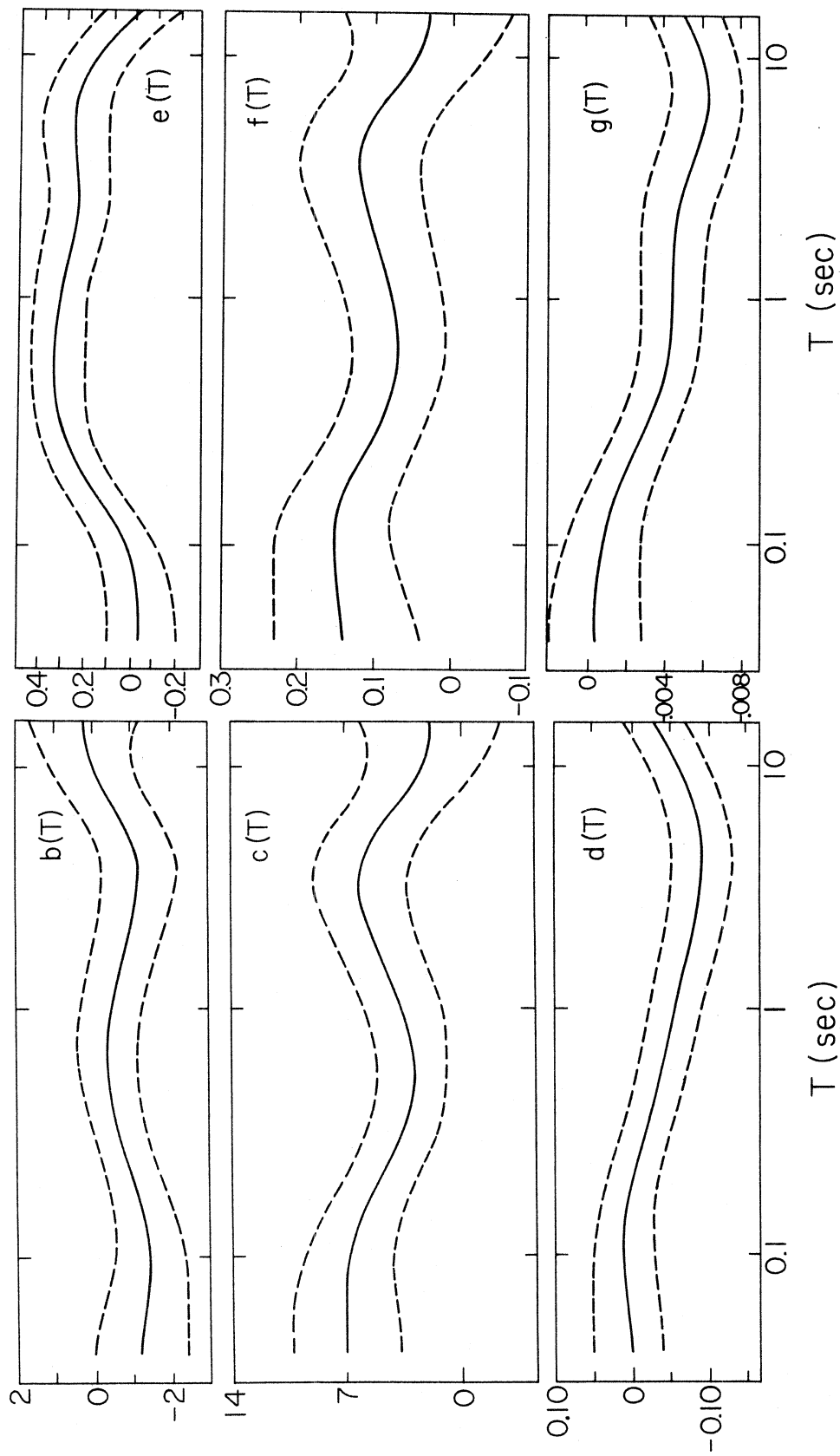


Figure 1

TABLE Ia

Regression Parameters for Equation (1)
and $\mu(T)$, $\sigma(T)$ at Eleven Selected Periods

Period,T(sec)	.040	.065	0.11	0.19	0.34	0.50
b(T)	-1.187	-1.310	-1.420	-1.065	-0.589	-0.414
c(T)	7.053	7.046	6.658	5.093	3.496	2.980
10*d(T)	0.044	0.074	0.102	0.015	-0.204	-0.364
e(T)	-0.047	-0.026	0.067	0.223	0.318	0.328
f(T)	0.137	0.146	0.154	0.126	0.089	0.074
1000*g(T)	-0.410	-0.495	-0.860	-1.939	-3.260	-4.014
$\mu(T)$	0.003	0.012	0.020	0.010	0.001	-0.003
$\sigma(T)$	0.492	0.468	0.435	0.391	0.367	0.368
Period,T(sec)	0.90	1.60	2.80	4.40	7.50	
b(T)	-0.467	-0.734	-1.079	-1.058	-0.338	
c(T)	3.369	4.572	5.856	5.722	3.342	
10*d(T)	-0.528	-0.654	-0.822	-0.876	-0.754	
e(T)	0.323	0.273	0.229	0.249	0.217	
f(T)	0.075	0.089	0.115	0.119	0.070	
1000*g(T)	-4.525	-4.548	-4.991	-5.712	-6.227	
$\mu(T)$	0.003	0.033	0.078	0.089	0.046	
$\sigma(T)$	0.380	0.400	0.444	0.465	0.455	

TABLE Ib

 $\log_{10}A_0(R)$ Versus Epicentral Distance R*

R (km)	$-\log_{10}A_0(R)$	R (km)	$-\log_{10}A_0(R)$	R (km)	$-\log_{10}A_0(R)$
0	1.400	140	3.230	370	4.336
5	1.500	150	3.279	380	4.376
10	1.605	160	3.328	390	4.414
15	1.716	170	3.378	400	4.451
20	1.833	180	3.429	410	4.485
25	1.955	190	3.480	420	4.518
30	2.078	200	3.530	430	4.549
35	2.199	210	3.581	440	4.579
40	2.314	220	3.631	450	4.607
45	2.421	230	3.680	460	4.634
50	2.517	240	3.729	470	4.660
55	2.603	250	3.779	480	4.685
60	2.679	260	3.828	490	4.709
65	2.746	270	3.877	500	4.732
70	2.805	280	3.926	510	4.755
80	2.920	290	3.975	520	4.776
85	2.958	300	4.024	530	4.797
90	2.989	310	4.072	540	4.817
95	3.020	320	4.119	550	4.835
100	3.044	330	4.164	560	4.853
110	3.089	340	4.209	570	4.869
120	3.135	350	4.253	580	4.885
130	3.182	360	4.295	590	4.900

* Only the first two digits may be assumed to be significant.

0.9 and smoothed along the T axis, are plotted in Figure 2. The smooth surface $p^*(\epsilon, T)$ thus represents the distribution of data ($FS(T)$ computed from recorded accelerograms) about the estimate $\hat{FS}(T)$ in (1). By fitting $p(\epsilon, T)$ in (4) to $p^*(\epsilon, T)$ at 91 periods, the average and standard deviation of the assumed normal distribution function can be evaluated. Their smoothed amplitudes are shown in Figure 3. The top portion of this figure shows that $\sigma(T)$ fluctuates between 0.35 and 0.5. For periods shorter than 1 sec, $\mu(T)$ is less than 0.02. Near $T=5$ sec, it reaches the local maximum of about 0.09.

To test the quality of fit of $p(\epsilon, T)$ to $p^*(\epsilon, T)$, Kolmogorov-Smirnov (K-S) and the χ^2 tests of the hypothesis that $p^*(\epsilon, T)$ can be approximated by a normal distribution $p(\epsilon, T)$ have been performed. The two full curves in the bottom part of Figure 3 show the computed χ^2 and K-S amplitudes. The dashed line (for χ^2 test) and the arrow (for K-S test) show the acceptance criteria at 95% confidence level (the jump in dashed line for $T > 10$ sec results from smaller data sample in this period range). It is seen that with a minor exception for periods $3 < T < 10$ sec in the χ^2 test, both K-S and χ^2 tests show that $p(\epsilon, T)$ in (4) represent an acceptable approximation to $p^*(\epsilon, T)$.

Following the discussion of Trifunac (1976a), it is also assumed in this work that $\log_{10} FS(T)$ as given by (1) applies only in the range $M_{\min} \leq M \leq M_{\max}$ where $M_{\min} = -b(T)/(2f(T))$ and $M_{\max} = (1-b(T))/(2f(T))$. For $M \leq M_{\min}$ the magnitude for which $FS(T)$ is sought is used only in the first term, M , in equation (1), while in terms $b(T)M$ and $f(T)M^2$, M_{\min} is used. For $M \geq M_{\max}$, M_{\max} is used in all terms in equation (1). This results in linear growth of $\log_{10}[FS(T)]$ with M for $M \leq M_{\min}$, in parabolic growth

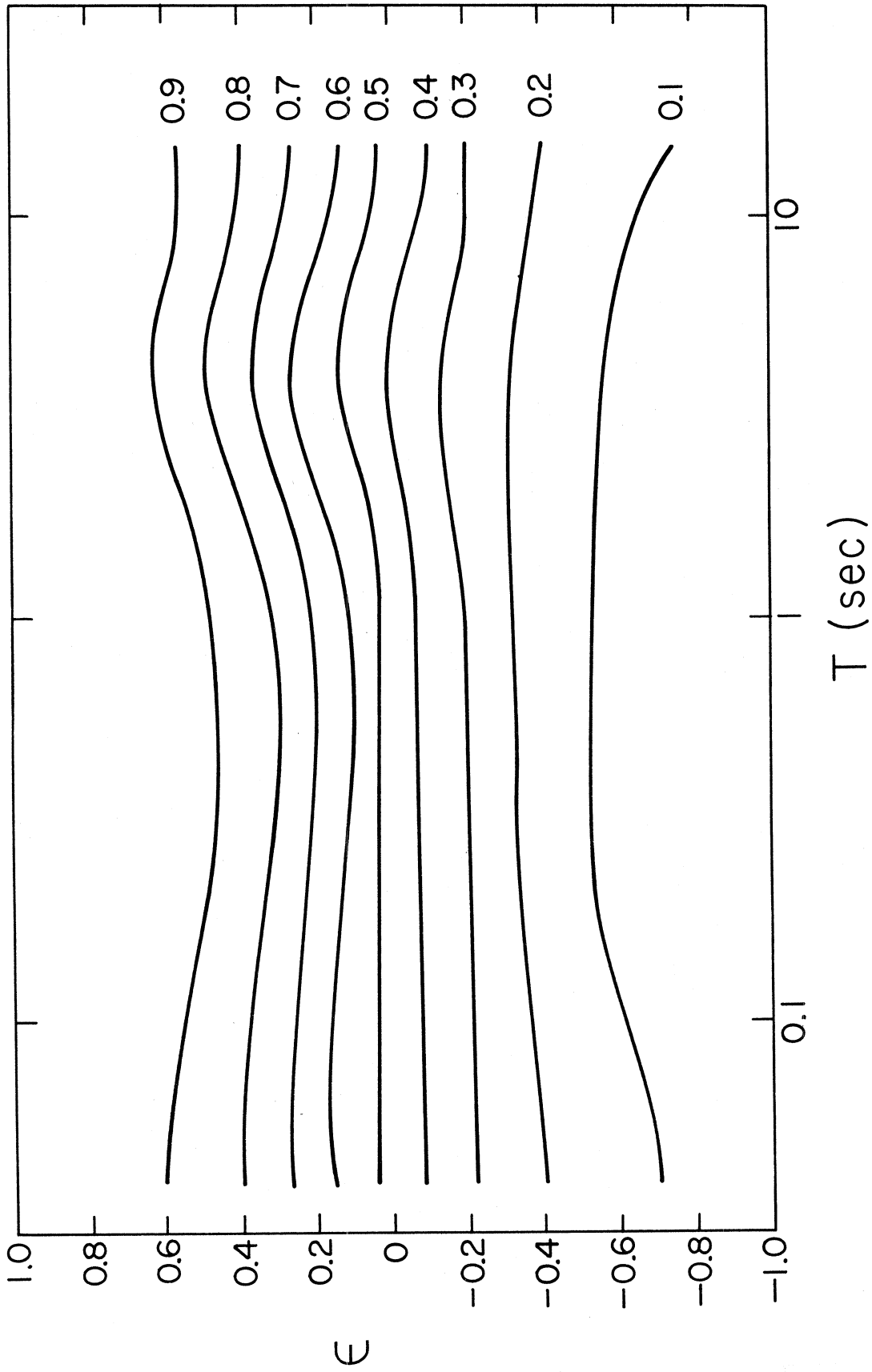


Figure 2

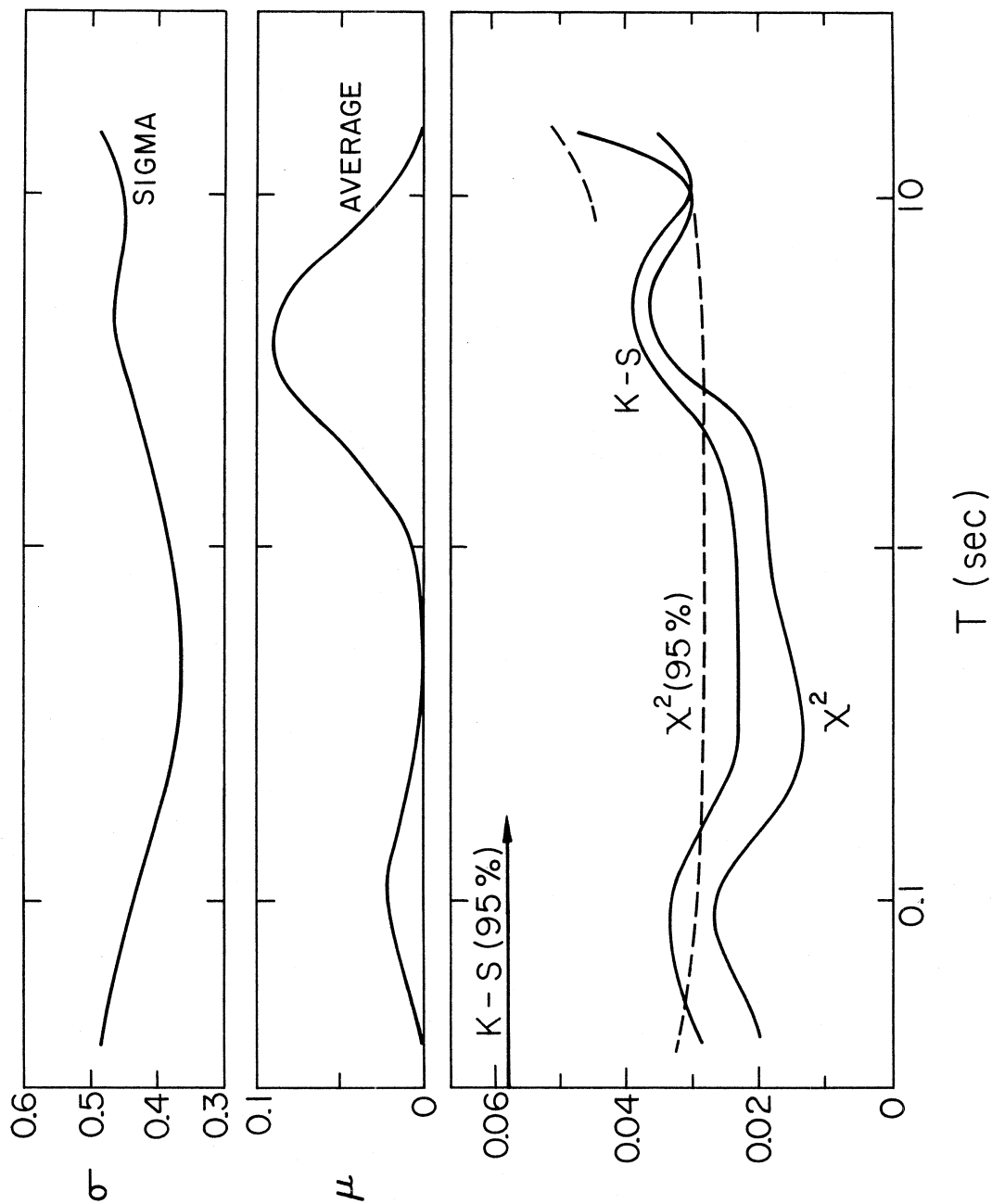


Figure 3

for $M_{\min} \leq M \leq M_{\max}$ and in constant $FS(T)$ corresponding to M_{\max} for all $M \leq M_{\max}$. Figure 4 shows M_{\min} and M_{\max} plotted versus T . It is seen that the present analysis suggests that the maximum amplitudes of strong motion in the high frequency range are reached for $M \sim 7.5$. For periods longer than about 0.15 sec, this maximum magnitude is greater than 8.

Figures 5 and 6 present examples of $FS(T)$ computed for $M = 4.5, 5.5, 6.5$ and 7.5 , at $R = 0$, for $p(\epsilon, T) = 0.5$, and for the spectral amplitudes which are greater than the spectra of recording and processing noise (Trifunac, 1976a). These examples show that the effect of the depth of sediments beneath the recording station is negligible for $T < 0.1$ sec. For periods longer than 0.2 to 0.3 sec, $FS(T)$ amplitudes are progressively greater on deep sediments. Near the period $T = 5$ sec, the logarithm of spectral amplitudes increases by about 0.09 (factor of 1.23 on the linear scale) per 1 km of depth of sediments. Figure 7 illustrates the attenuation of spectral amplitudes with epicentral distance for horizontal and vertical accelerations and for $h = 2$ km, $M = 6.5$ and $p(\epsilon, T) = 0.5$.

Figure 8 presents the Fourier spectrum amplitudes computed from equation (1) for $p = 0.1, 0.5$ and 0.9 , $M = 6.4$, $h = 19,500$ ft, $R = 15$ km and for horizontal ground motion. Superimposed on the same scale are the NS (full lines) and EW (dotted lines) Fourier amplitude spectra of strong ground motion recorded during the Imperial Valley, California, earthquake of 1940, and corresponding to the same numerical values of M , R , and h . It is seen that the average spectral amplitudes (continuous curve for $p = 0.5$) approximate the recorded spectral amplitudes well. Figure 9 presents another example of such comparison for the Fourier spectra computed

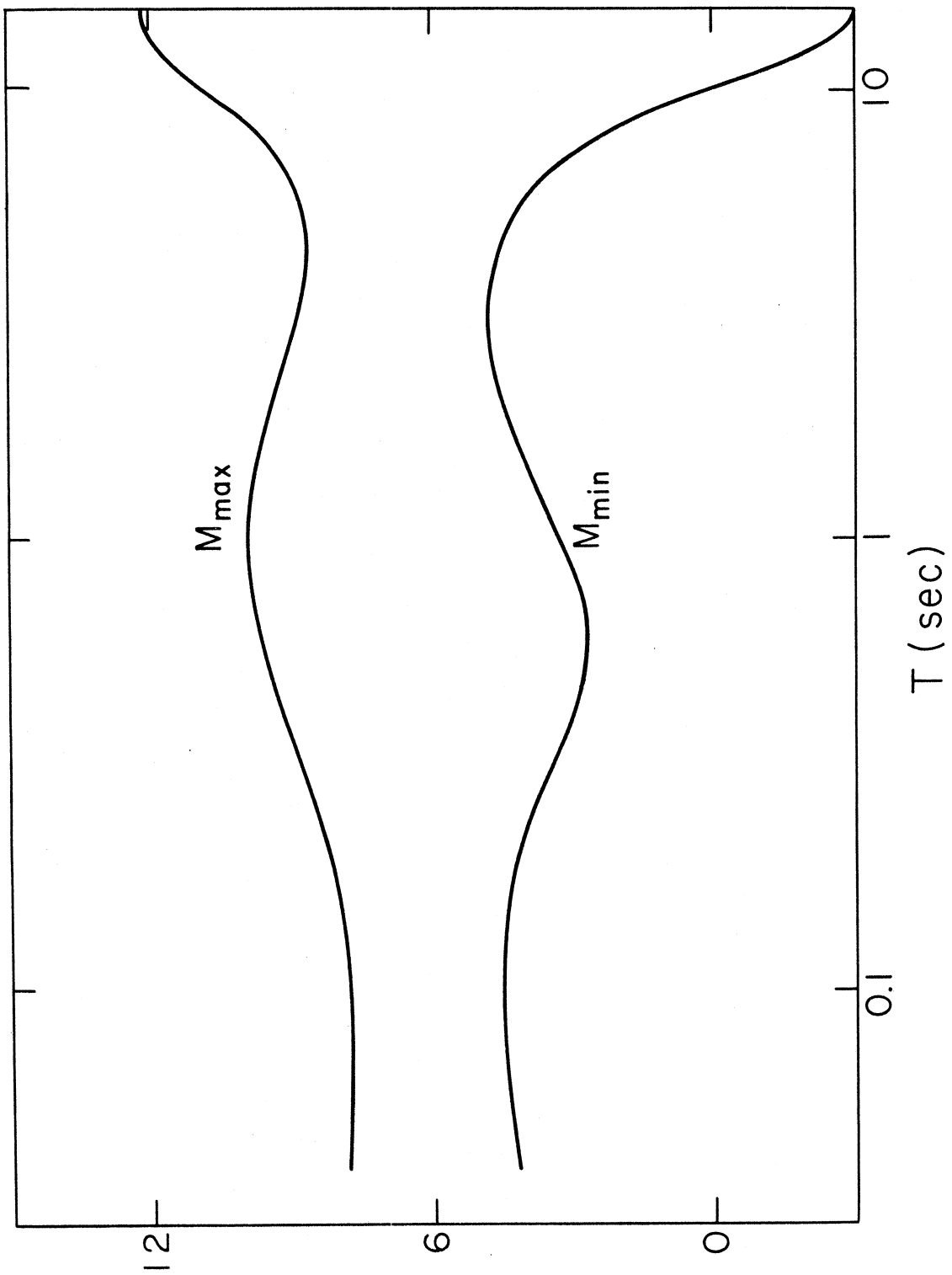


Figure 4

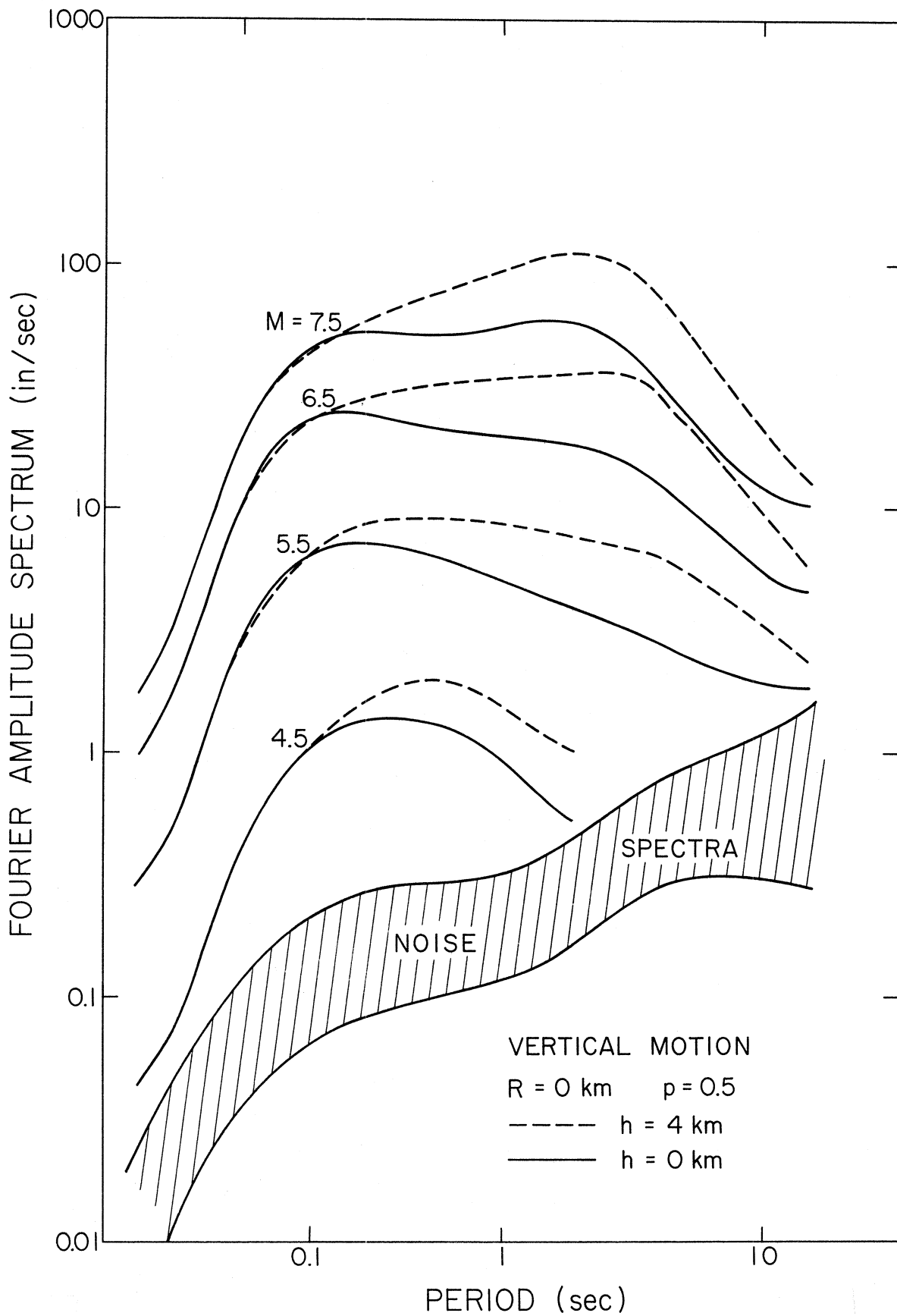
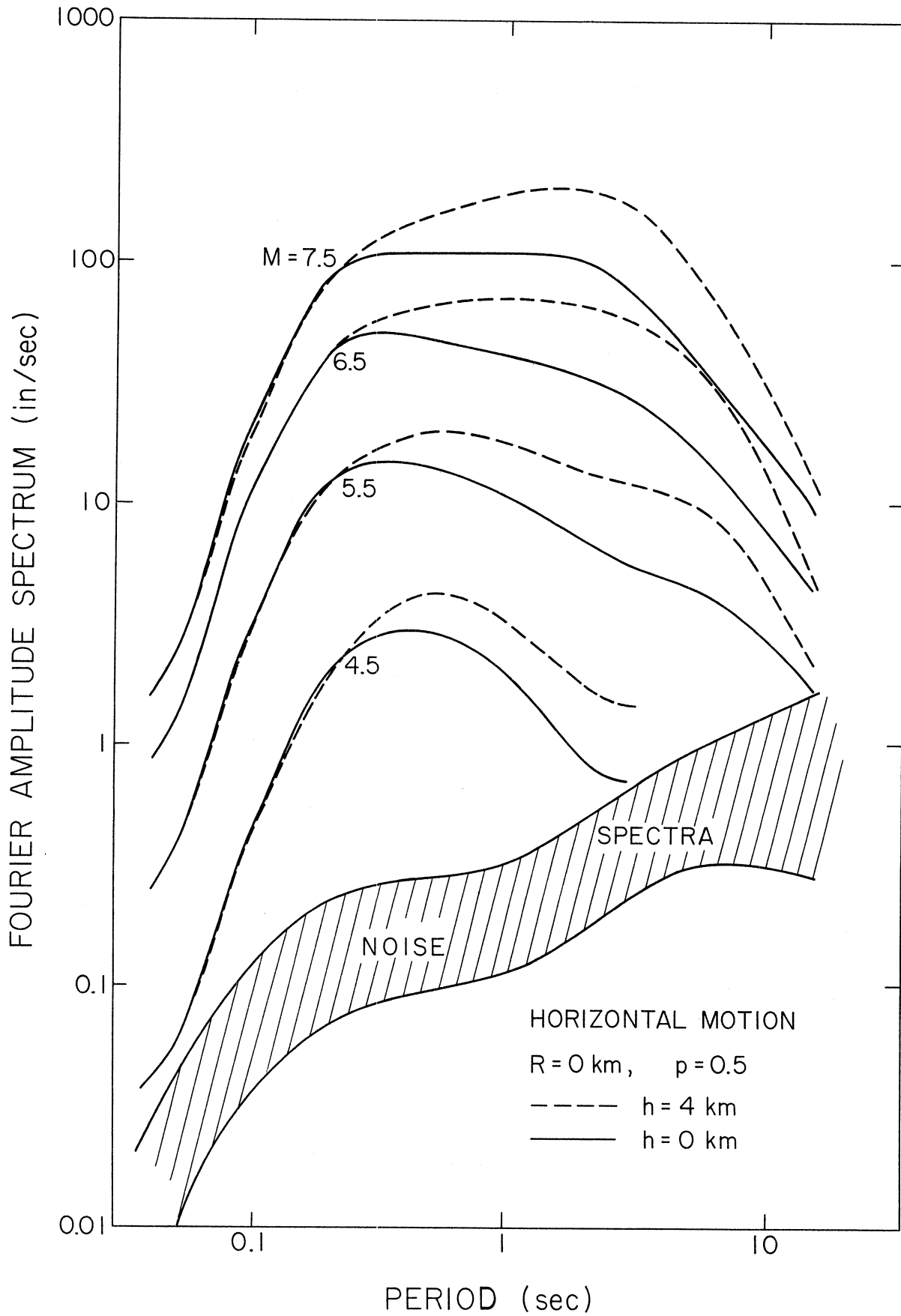


Figure 5



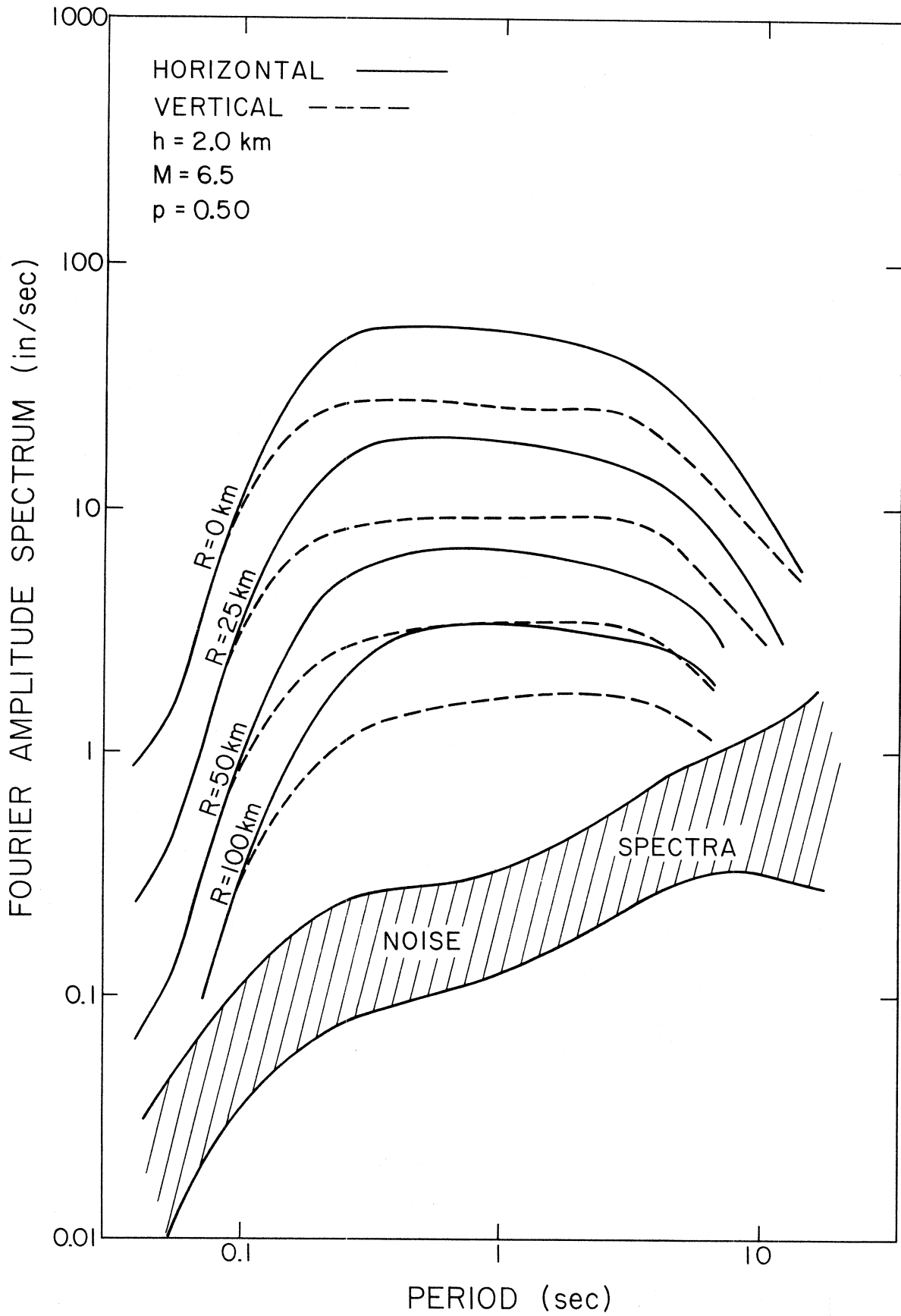


Figure 7

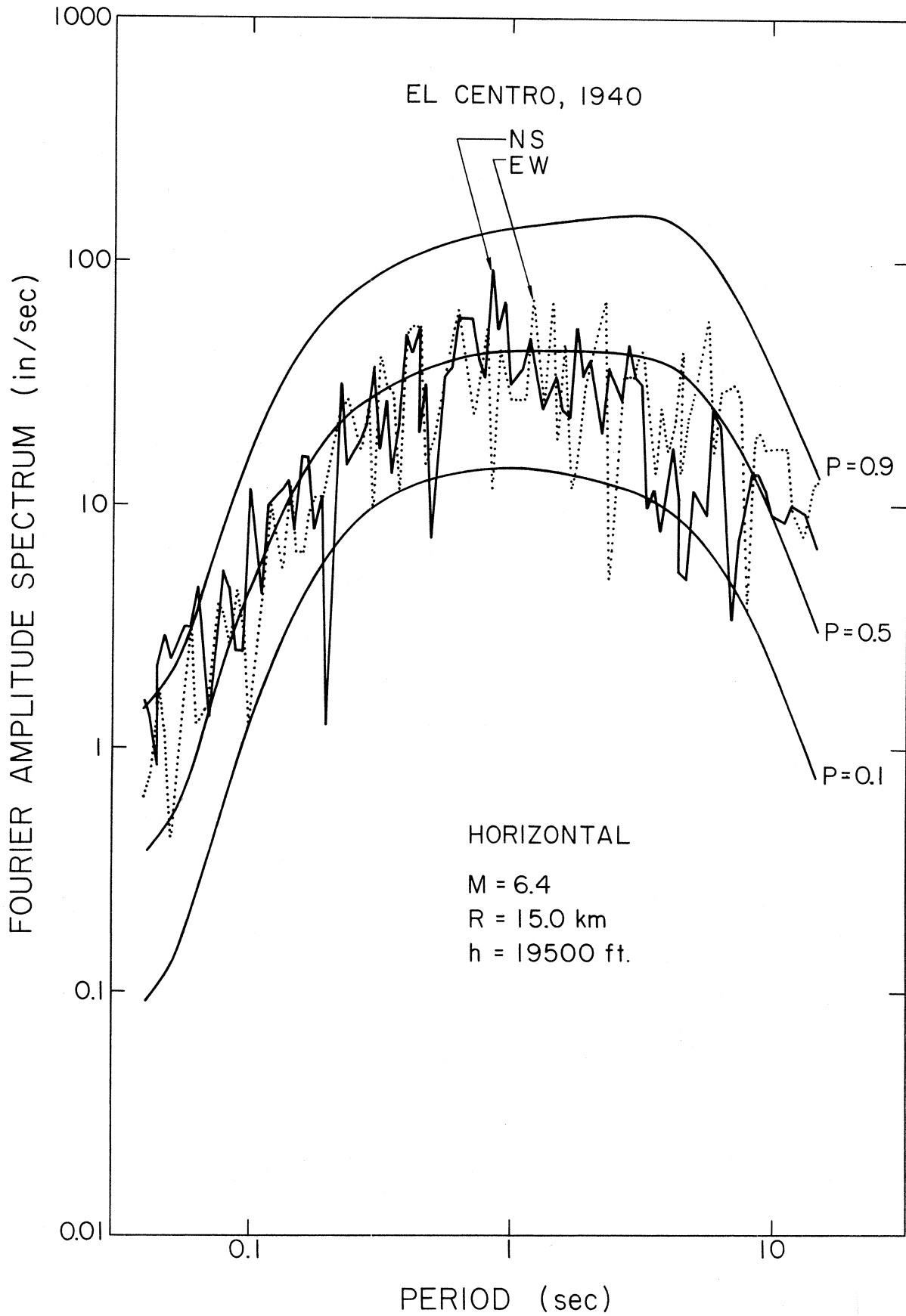


Figure 8

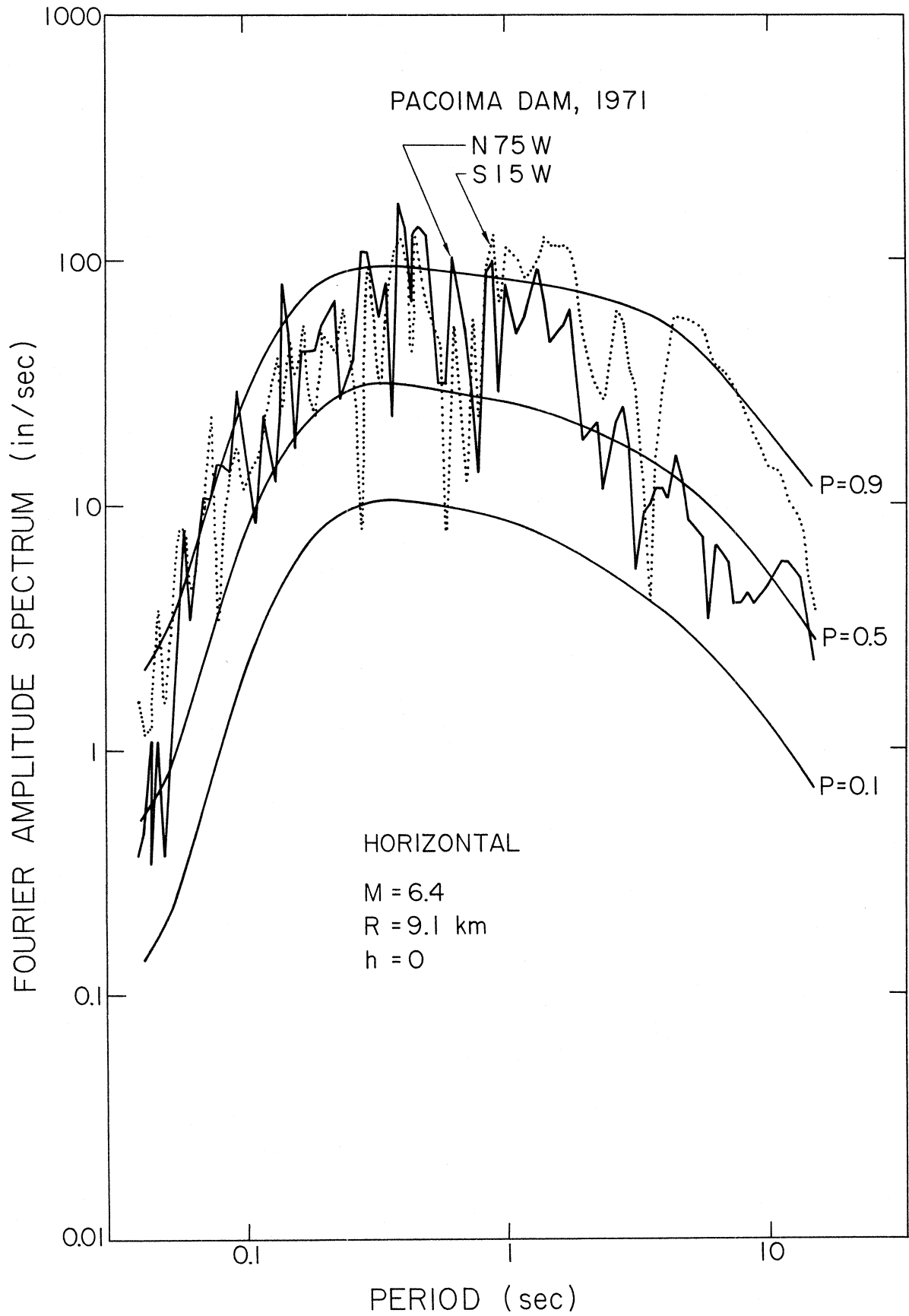


Figure 9

from the Pacoima Dam accelerograms recorded during the February 9, 1971 earthquake in San Fernando, California.

SCALING OF FOURIER AMPLITUDE SPECTRA IN TERMS
OF MMI, h AND v

For scaling of Fourier amplitude spectra in terms of the expected Modified Mercalli Intensity (MMI) at the site, I_{MM} , depth of sediments beneath the site, h , and the direction of strong shaking ($v=0$ for horizontal and $v=1$ for vertical motions) we use the functional form analogous to that proposed by Trifunac (1978b),

$$\log_{10}[FS(T)] = b(T)I_{MM} + c(T) + d(T)h + e(T)v \quad . \quad (5)$$

In agreement with the preceding analogous work involving the same data base and the scaling in terms of MMI (Trifunac and Brady, 1975; Trifunac, 1976b; Trifunac, 1978b), we intentionally delete any explicit dependence of amplitudes of $FS(T)$ in (5) on epicentral distance. It is clear that such dependence would diminish the uncertainty associated with the estimated $FS(T)$ from the empirical equation (5) by reducing the standard deviation of observed relative to the estimated $FS(T)$. However, at the same time, such dependence would model explicitly the amplitude attenuation of strong shaking in California and would thus formally render equation (5) not applicable to other parts of the United States and the world, where the nature of wave attenuation is different. Eliminating the explicit dependence of equation (5) on the epicentral distance R increases the uncertainty of the estimated $FS(T)$ but permits one to use this equation formally in the seismic regions where MMI at the site can be estimated by other independent means. Recent comparison of such approach (Anderson, 1979) with the independent estimates of the amplitudes of strong shaking in terms of earthquake magnitude and epicentral distance has shown that even without an explicit dependence of $FS(T)$ on R , the

end seismic risk results are reasonable. This is based on a comparison of amplitudes of shaking with fixed return period using the scaling equivalent of equation (5) (Trifunac, 1978b) for MMI and the scaling equivalent of equation (1) for magnitudes, but with the site parameter s instead of depth h .

The estimates of $b(T)$, $c(T)$, $d(T)$ and $e(T)$, denoted by $\hat{b}(T)$, $\hat{c}(T)$, $\hat{d}(T)$ and $\hat{e}(T)$ have been computed from the least squares fit of equation (5) to the data on $FS(T)$ amplitudes at 91 periods. The method of data selection, minimization of the degree to which abundantly recorded earthquakes could bias the estimates of $\hat{b}(T)$, ..., and $\hat{e}(T)$ and the details of regression analysis are identical to those proposed by Trifunac (1978b) and need not be repeated here.

The residuals are

$$\varepsilon(T) = \log_{10}[FS(T)] - \log_{10}[\hat{FS}(T)] \quad , \quad (6)$$

where $FS(T)$ is the Fourier amplitude spectrum computed from recorded accelerograms, and $\hat{FS}(T)$ represents the estimates based on equation (5) and scaling functions $\hat{b}(T)$, ..., and $\hat{e}(T)$. These residuals characterize the uncertainties associated with the use of equation (5). As for the scaling of $FS(T)$ in terms of M , R , h and v , we assume here that $\varepsilon(T)$ can be described by a normal distribution in terms of $\mu(T)$ and $\sigma(T)$ as in equation (4).

Figure 10 shows $\hat{b}(T)$, $\hat{c}(T)$, $\hat{d}(T)$ and $\hat{e}(T)$ (full lines) and the estimates of the associated 95% confidence intervals (dashed lines). Table II presents the same functions together with $\mu(T)$ and $\sigma(T)$ (for use in equation (4)) at eleven selected periods.

The probability $p^*(\varepsilon, T)$, that $\varepsilon(T)$ will not be exceeded is shown in

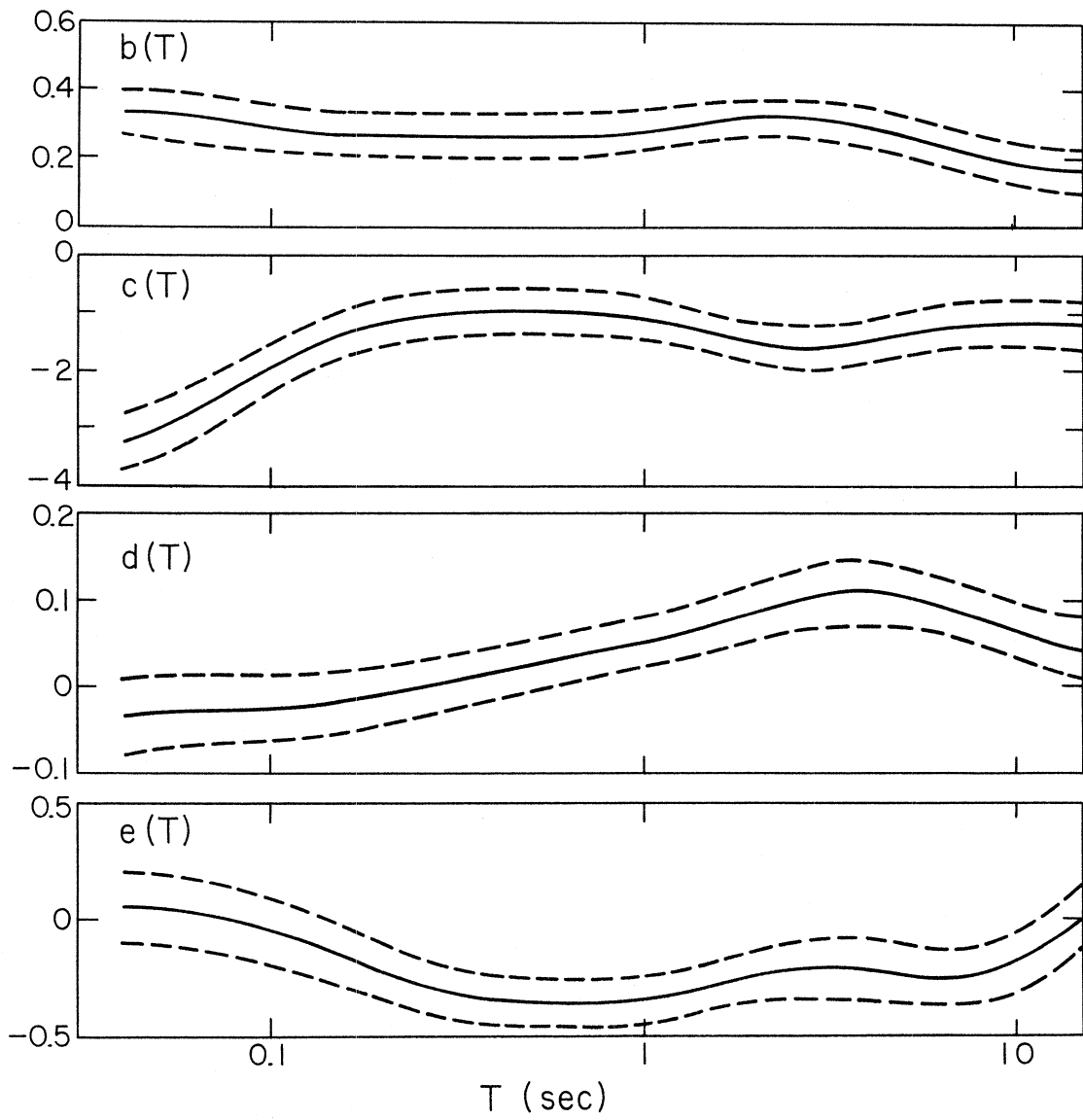


Figure 10

TABLE II

Regression Parameters for Equation (5)
and $\mu(T)$, $\sigma(T)$ at Eleven Selected Periods

Period, T(sec)	.040	.065	0.11	0.19	0.34	0.50
b(T)	0.340	0.319	0.286	0.270	0.268	0.266
c(T)	-3.200	-2.659	-1.726	-1.171	-0.984	-0.944
$10*d(T)$	-0.337	-0.298	-0.236	-0.078	0.132	0.260
e(T)	0.039	0.020	-0.075	-0.231	-0.329	-0.348
$\mu(T)$	-0.069	-0.052	-0.028	-0.021	-0.018	-0.016
$\sigma(T)$	0.581	0.577	0.544	0.470	0.410	0.397
Period, T(sec)	0.90	1.60	2.80	4.40	7.50	
b(T)	0.283	0.314	0.319	0.282	0.214	
c(T)	-1.096	-1.437	-1.590	-1.421	-1.137	
$10*d(T)$	0.478	0.744	1.010	1.060	0.806	
e(T)	-0.340	-0.264	-0.201	-0.233	-0.243	
$\mu(T)$	-0.010	0.001	0.012	0.013	-0.005	
$\sigma(T)$	0.405	0.436	0.483	0.497	0.470	

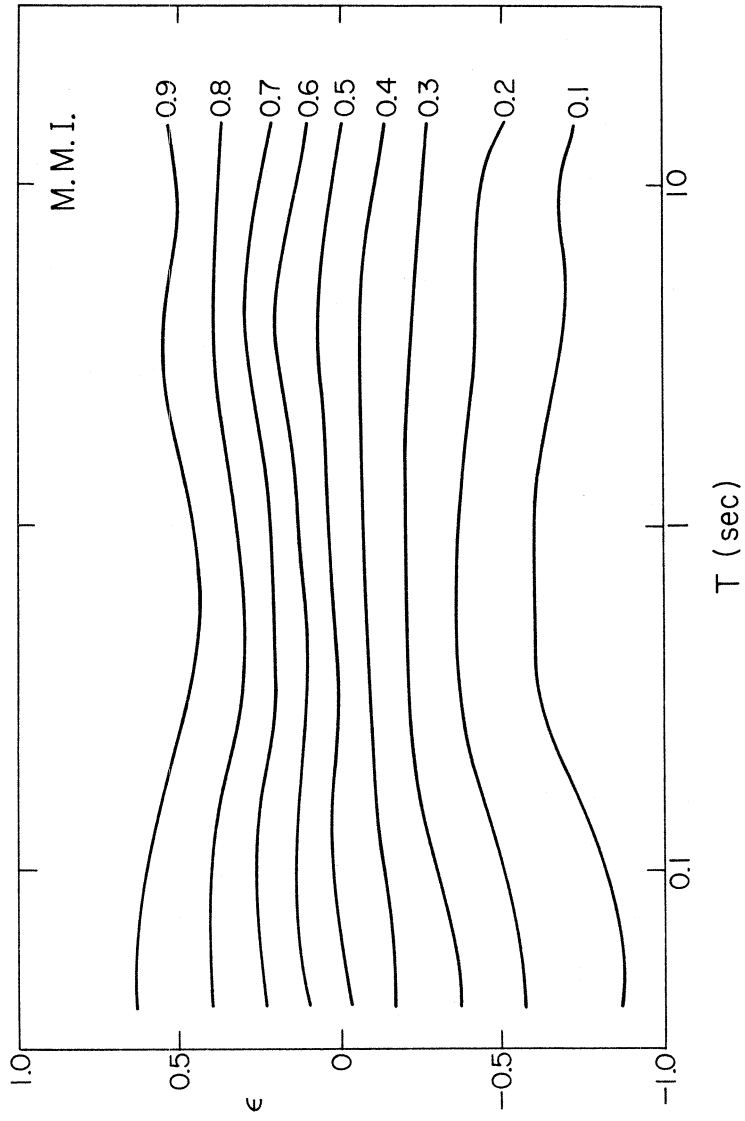


Figure 11

Figure 11. The smoothed surface described by $p^*(\epsilon, T) = 0.1, 0.2, \dots, 0.8$ and 0.9 represents the distribution of $FS(T)$ data computed from recorded accelerograms relative to the estimates $\hat{FS}(T)$. Functions $\mu(T)$ and $\sigma(T)$ (top and middle of Figure 12) in equation (4), least squares fitted to the data on $p^*(\epsilon, T)$ in Figure 11 then provide an analytical approximation $p(\epsilon, T)$ to $p^*(\epsilon, T)$.

To test the adequacy of $p(\epsilon, T)$ in (4) as an approximation to $p^*(\epsilon, T)$ in Figure 11, χ^2 and Kolmogorov-Smirnov (K-S) tests of the quality of fit were carried out. As Figure 12 (bottom) shows, computed χ^2 (continuous curve) was larger than the acceptable χ^2 at the 95% confidence level (dashed line). Computed (K-S) differences were always smaller than the permissible (K-S) difference at the 95% confidence level. However, the overall quality of the fit was judged acceptable and $\mu(T)$ and $\sigma(T)$ were adopted with $p(\epsilon, T)$ in equation (4) as useful approximation to $p^*(\epsilon, T)$.

Figures 13 and 14 present examples of Fourier amplitude spectra plotted for MMI levels IV, VI, VIII, X and XII, for vertical and horizontal motions, $p(\epsilon, T) = 0.5$ and $h = 0$ and 4 km. These spectral amplitudes have been computed from equation (5) via equations (6) and (4) and can be considered representative of the observed shaking for MMI up to about VIII. The curves plotted for MMI = X and for XII are presented for completeness only and at the present time, represent only an extrapolation based on the data for smaller intensities.

Figures 15 and 16 show examples of a comparison between the estimated (continuous smooth lines) and the Fourier spectrum amplitudes computed from recorded accelerograms (irregular full line and dotted line).

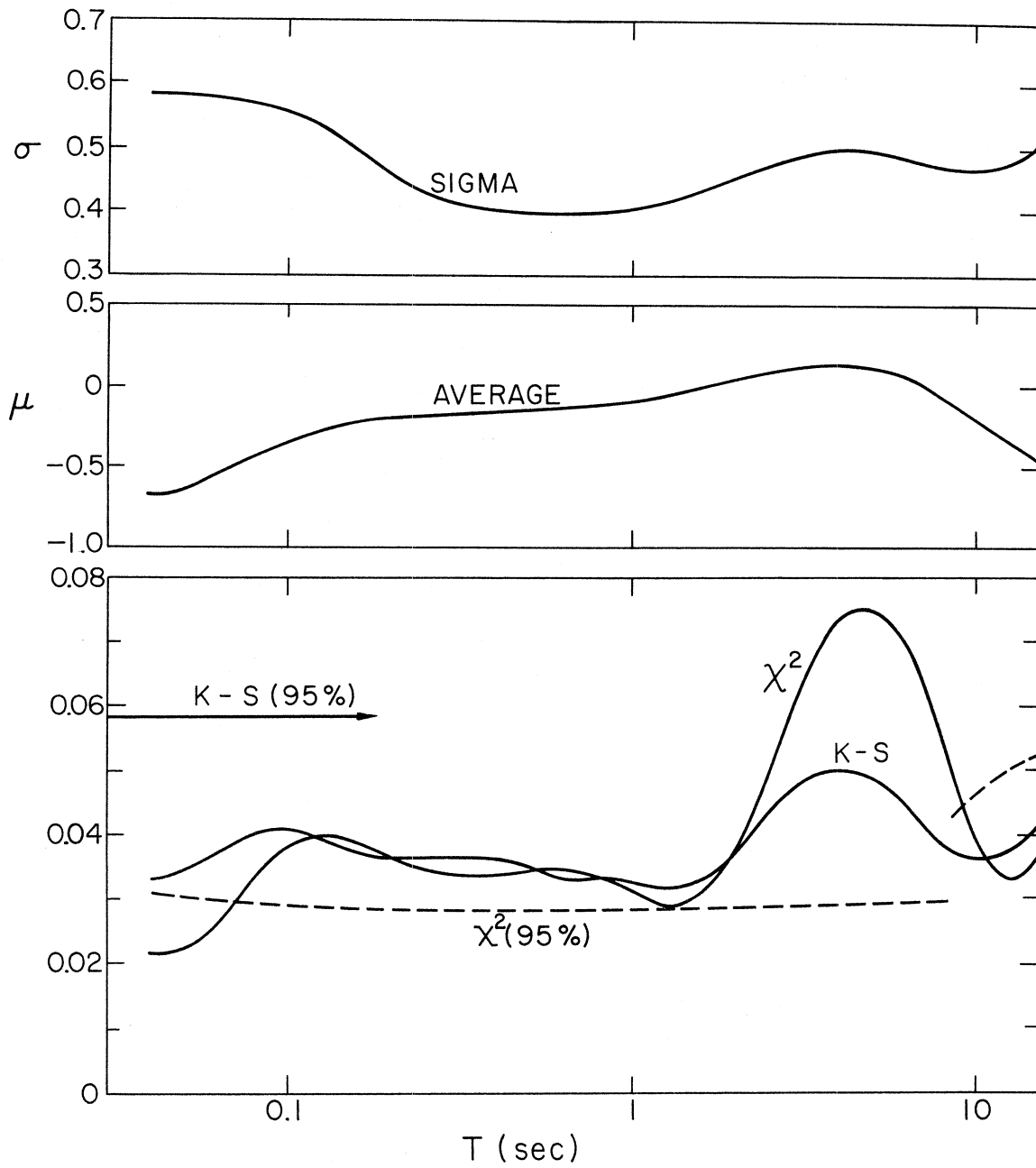


Figure 12

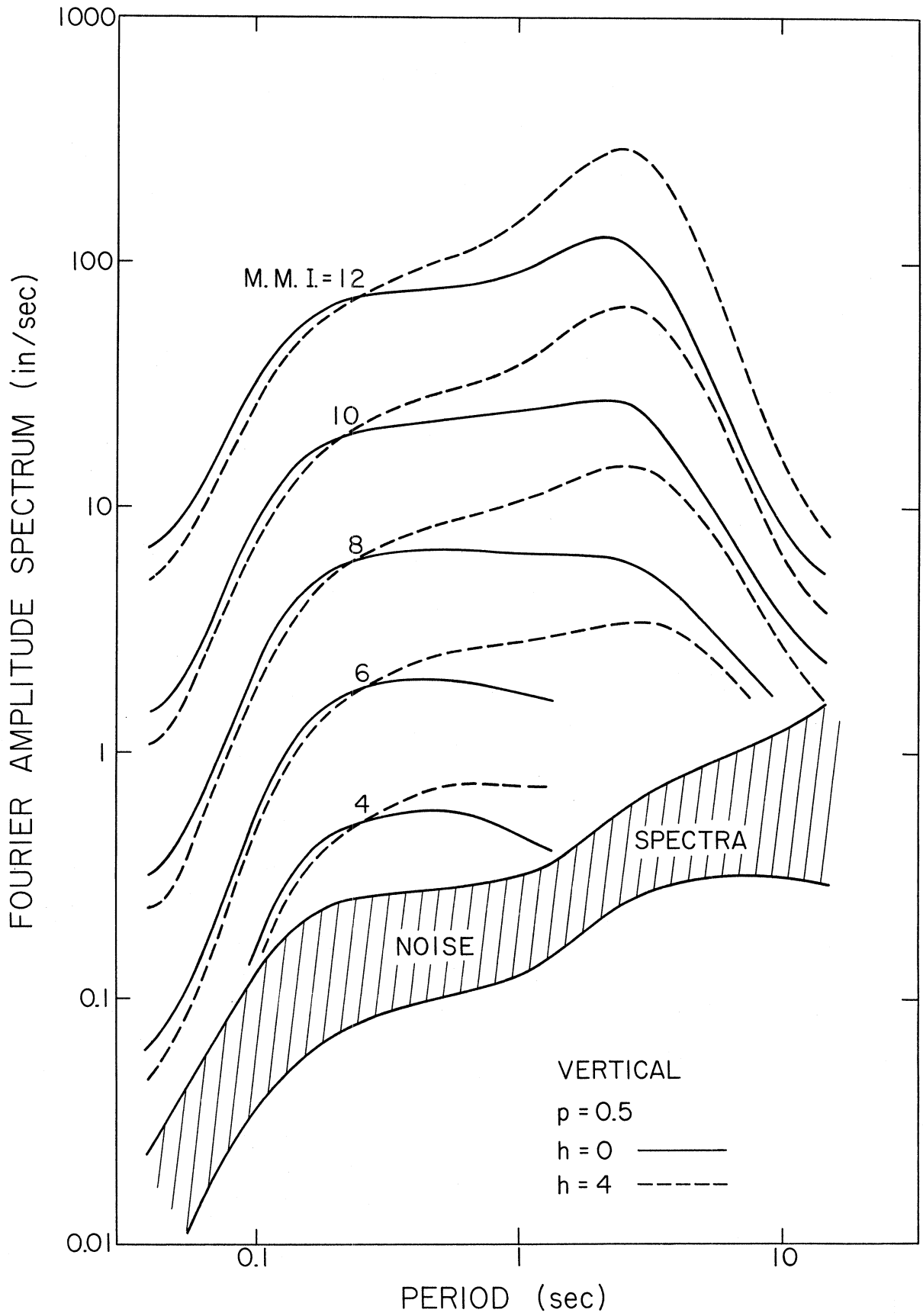


Figure 13

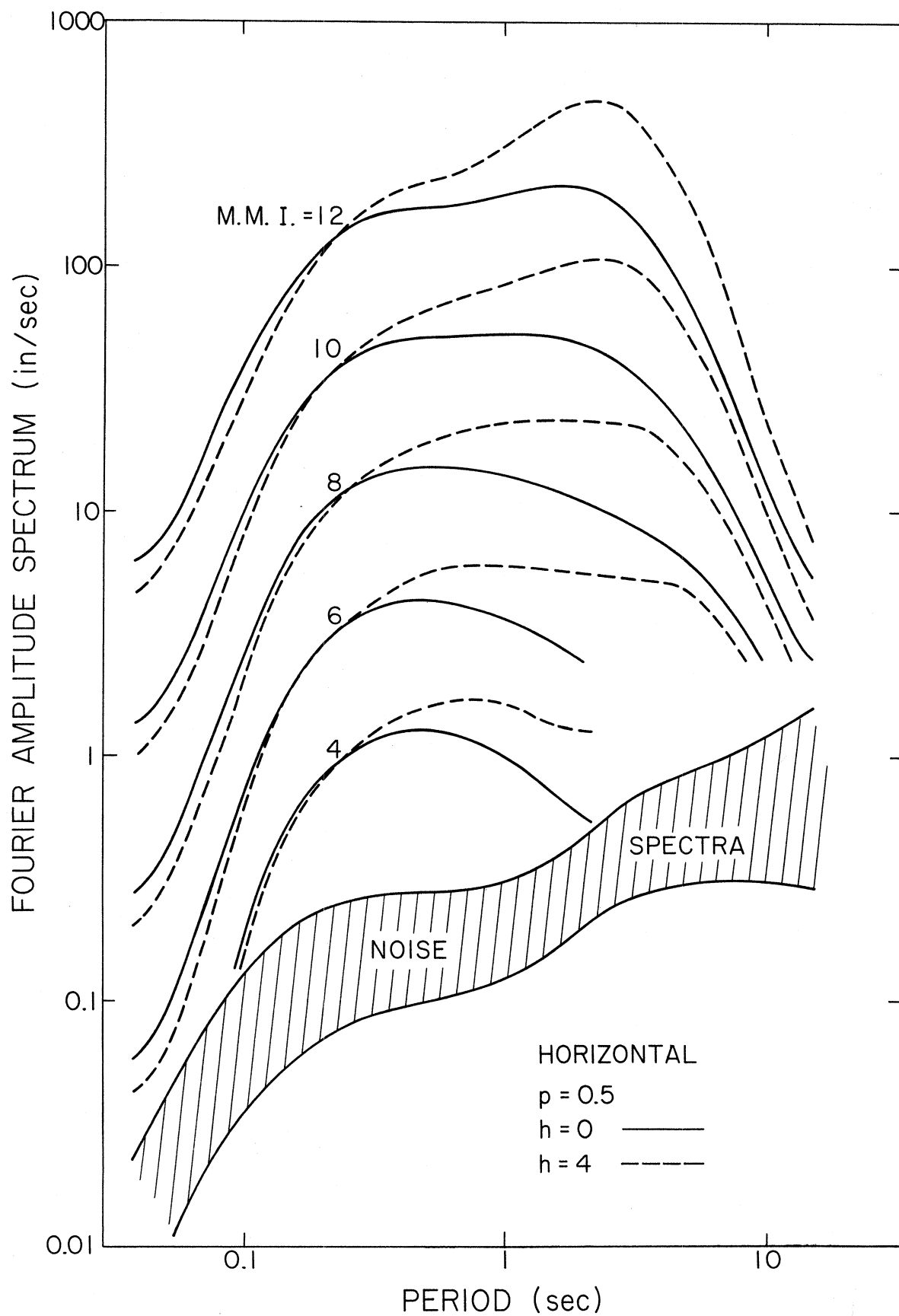


Figure 14

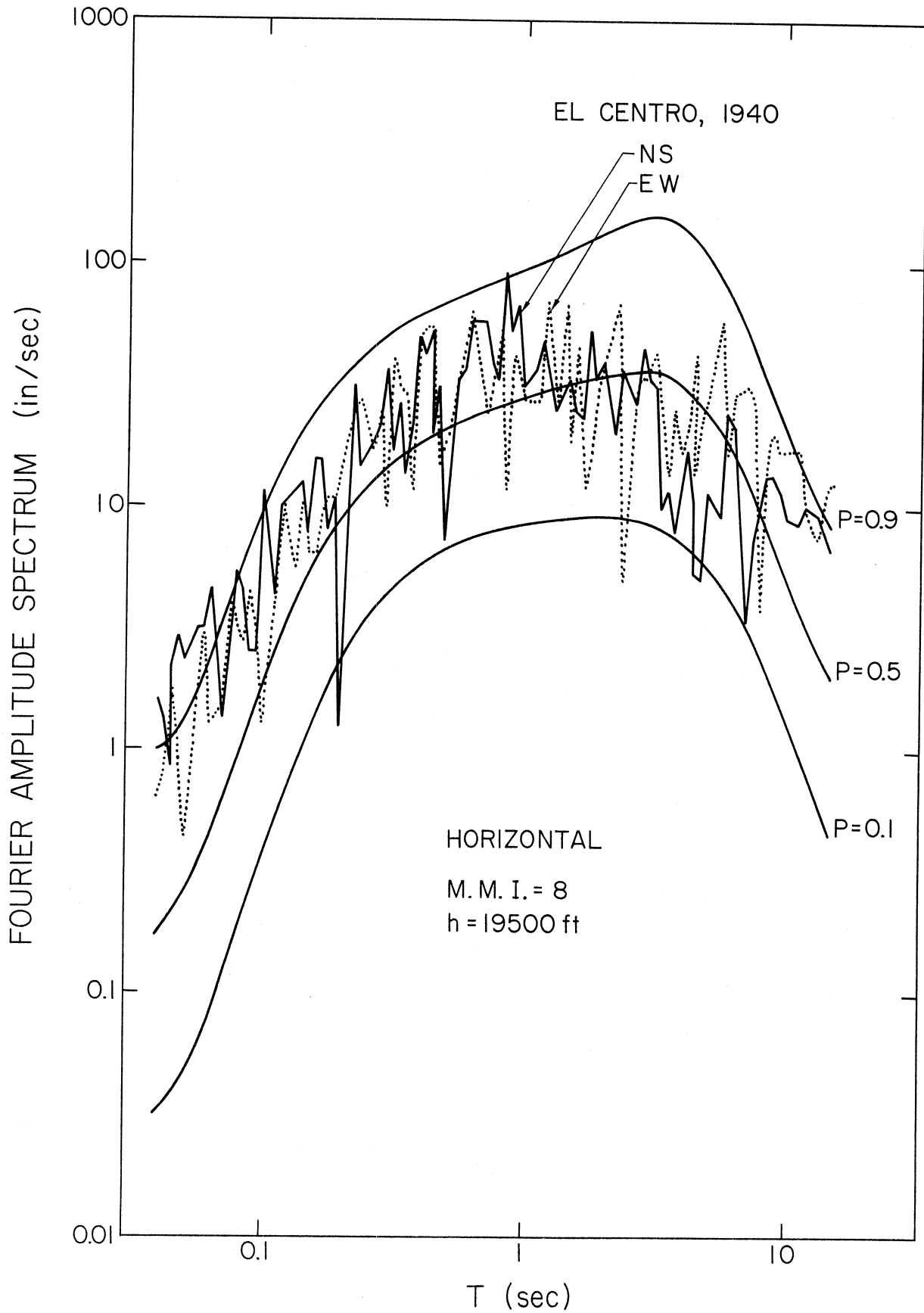


Figure 15

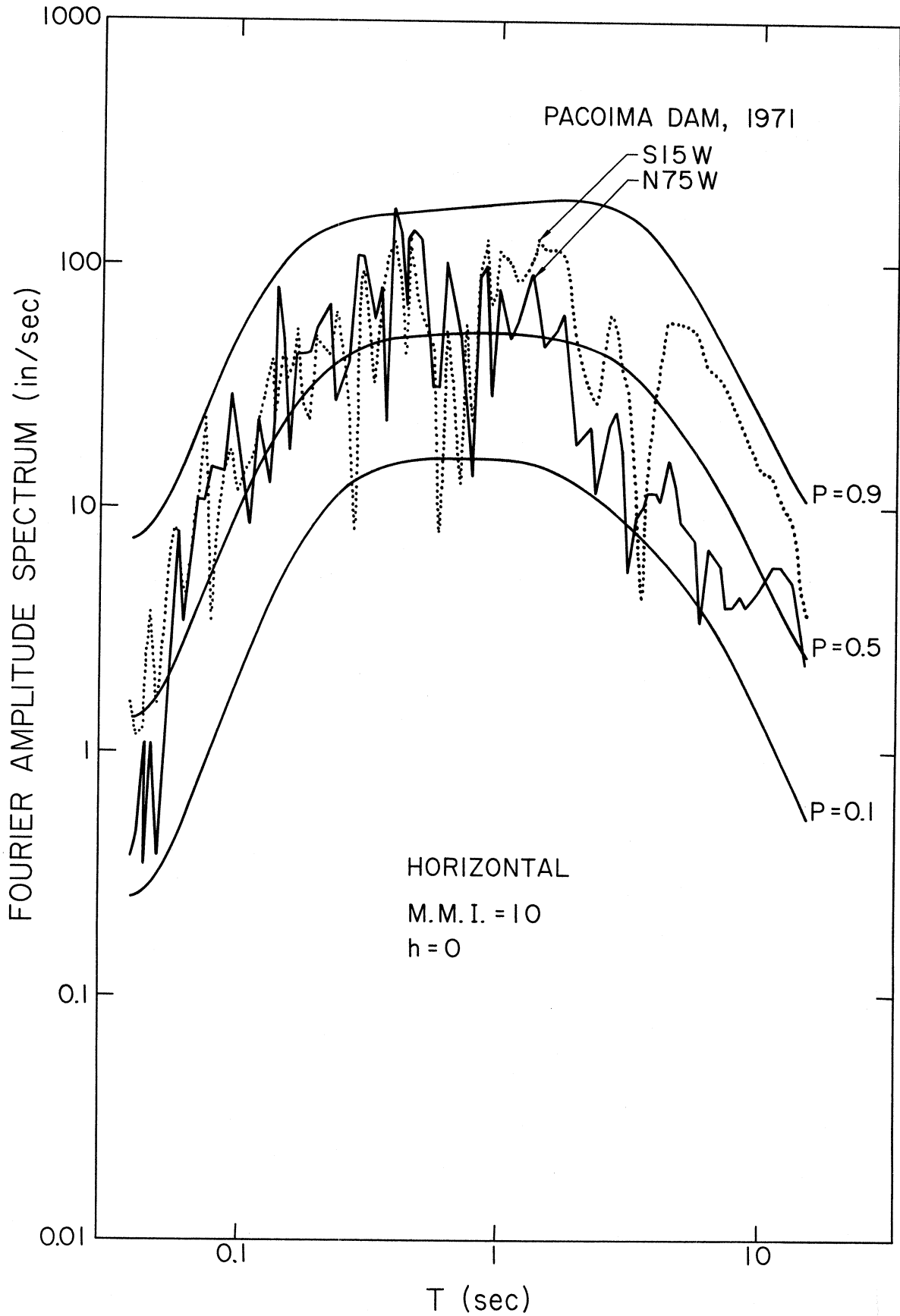


Figure 16

Figure 15 illustrates a site on deep sediments (Imperial Valley, 1940, earthquake recorded in El Centro). In Figure 16, such comparison is made for a rock site ($h=0$) near Pacoima Dam and for the Fourier amplitude spectra of accelerations recorded during the San Fernando, California, earthquake of 1971.

The trends of $b(T)$, $c(T)$, $d(T)$, and $e(T)$ versus T in Figure 10 are quite similar to the trends of the corresponding functions used by Trifunac (1978b) for the scaling of Fourier amplitude spectra in terms of the rough site classification $s=0, 1$ and 2 . Detailed analysis of the resulting spectral amplitudes (e.g., Figures 5, 6, 13 and 14) shows better internal consistency between the models in equations (1) and (5) in this work than between the corresponding models in Trifunac (1976a) and Trifunac (1978b), which were based on $s=0, 1$ and 2 site classifications. This can be attributed to the more uniform dependence of the regression models in equations (1) and (5) on the local site geology when modeled in terms of the depth of sediments h , than in terms of $s=0, 1$ or 2 . Since the distribution of the data, so far available, among $s=0, 1$ and 2 is 63%, 23% and 8%, respectively, it is seen that the present analysis which uses h leads to more uniform weighting of the site effects through $d(T)$.

As pointed out by Trifunac (1976b), the lack of data for $I_{MM} > VII$ and $I_{MM} < V$ prevents one from evaluating the adequacy of $b(T)$ for $I_{MM} > VIII$. Furthermore, the lack of a physical basis for assigning a linear numerical scale from 1 to 12 to the MMI levels, I_{MM} , in the range from I to XII makes it difficult to justify on any physical basis the linear term $b(T)I_{MM}$ in equation (5). In search of a simple empirical scaling

relationship between the logarithm of the amplitudes of strong shaking and the MMI levels arbitrarily assigned to a linear numerical scale, it has been found that a linear equation of the form reproduced in equation (5) often describes the trend of the data (Barosh, 1969; Trifunac, 1978b). Thus, from a practical viewpoint, it is useful to check the internal consistency between equations (1) and (5) in the range of MMI where data is now not available and to see to what extent such internal consistency might suggest the success in extrapolating the estimates of strong motion amplitudes in terms of equation (5). Figures 17 and 18 show this test where the spectral amplitudes extrapolated via equation (5) and for $MMI = XII$ are compared with the corresponding estimates of Fourier spectrum amplitudes based on equation (1). It can be seen that the spectra computed from equation (5) (dashed lines) for $p = 0.5$ are in general consistent with spectra computed from equation (1) (full lines) suggesting that the formalism used in equation (5) most probably leads to reasonable estimates of $FS(T)$ for $MMI > VIII$ and outside the range of MMI levels when this equation can be justified on the basis of the available data. Detailed comparison of these figures with the corresponding Figure 8 in Trifunac (1978b), which presents the same type of comparison for scaling in terms of the site classification, s , suggests that there exists better internal consistency between equations (1) and (5) in this analysis than between the corresponding models in Trifunac (1978b). This further suggests the improvement in the overall quality of the empirical scaling models which incorporate the effects of local site conditions through continuous variable h , relative to the models using rough site classification, s , only.

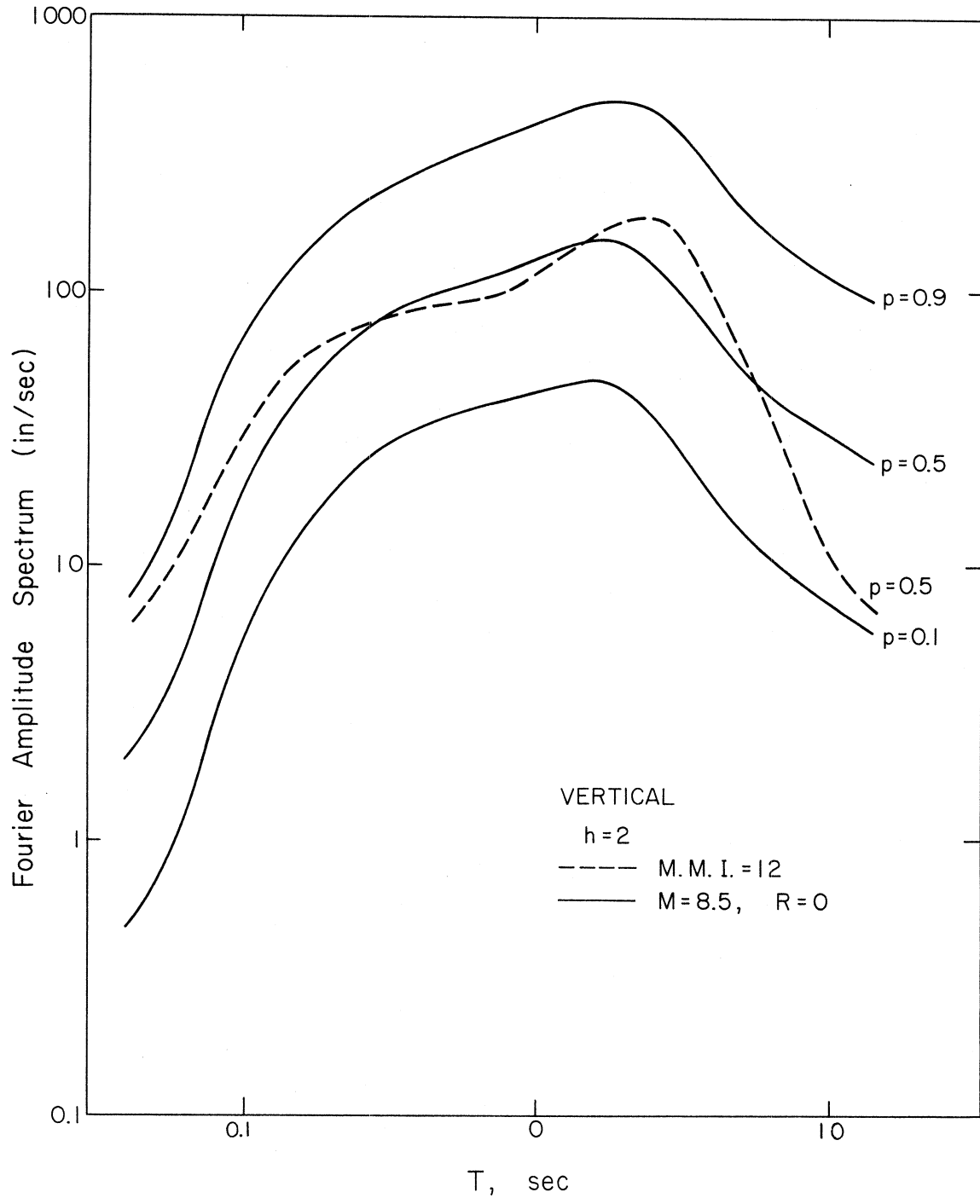


Figure 17

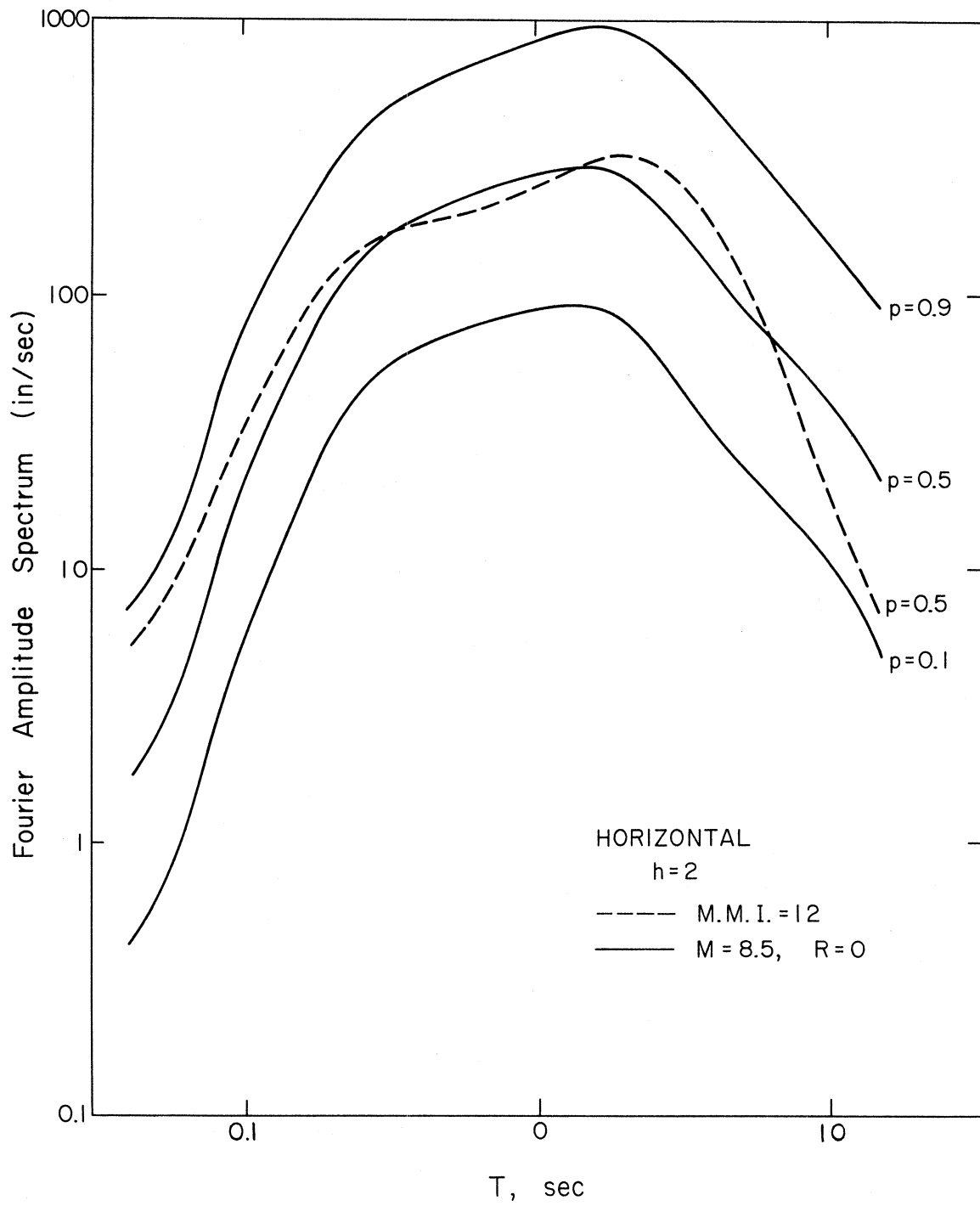


Figure 18

CONCLUSIONS

In this report we have presented an extension of the new method (Trifunac, 1976a; 1978b) for scaling of the Fourier amplitude spectra directly in terms of the earthquake magnitude and the MMI at the recording station. The form of the empirical scaling equation presented here is identical to the family of such equations presented previously for similar (Trifunac, 1976a; 1978b) and related estimation of spectral amplitudes (Trifunac and Anderson, 1977; 1978a,b) of strong earthquake ground motion. The improvement presented here results from a characterization of local geologic conditions in terms of the overall depth of sediments beneath the recording station.

It has been found that the Fourier spectrum amplitudes depend significantly on the depths of sediments beneath the recording station. For long period motions ($T > 1$ sec) spectral amplitudes increase by 0.1 on the logarithmic scale per km of depth, h . For short periods, $T < 0.1$ sec, this trend is reversed and spectral amplitudes diminish by less than 0.03 (on the logarithmic scale) per km of depth. Though consistent with all previous scaling of similar and related spectral amplitudes at high frequencies, and probably physically present, this trend is not significant when judged by simplistic 95% confidence intervals shown in Figures 1 and 10.

ACKNOWLEDGEMENTS

We thank J.G. Anderson, M. Dravinski and B. Westermo for critical reading of the text and for useful comments.

This work was supported in part by a contract from the U.S. Nuclear Regulatory Commission and by a grant from the National Science Foundation.

REFERENCES

- Anderson, J.G. (1979). Uniform Risk Fourier Amplitude Spectra Derived from Intensity Data on Earthquake Occurrence, NUREG/CR-0689, report from Civil Engineering Dept., U.S.C., to N.R.C.
- Barosh, P.J. (1969). Use of Seismic Intensity Data to Predict the Effects of Earthquakes and Underground Nuclear Explosions, Geol. Survey Bull. 1299.
- Seed, H.B., C. Ugas and J. Lysmer (1974). Site-Dependent Spectra for Earthquake-Resistant Design, Earthquake Eng. Res. Center, EERC 74-12, Univ. of California, Berkeley.
- Richter, C.F. (1958). Elementary Seismology, Freeman, San Francisco.
- Trifunac, M.D. (1976a). Preliminary Empirical Model for Scaling Fourier Amplitude Spectra of Strong Ground Acceleration in Terms of Earthquake Magnitude, Source to Station Distance and Recording Site Conditions, Bull. Seism. Soc. Amer., 66, 1343-1373.
- Trifunac, M.D. (1976b). A Note on the Range of Peak Amplitudes of Recorded Accelerations, Velocities and Displacements with Respect to the Modified Mercalli Intensity, Earthquake Notes, 47, 9-24.
- Trifunac, M.D. (1977). Forecasting the Spectral Amplitudes of Strong Earthquake Ground Motion, Sixth World Conf. Earthquake Eng., New Delhi, India.
- Trifunac, M.D. (1978a). Response Spectra of Earthquake Ground Motion, Proc. ASCE, EM5, Vol. 104, 1081-1097.
- Trifunac, M.D. (1978b). Preliminary Empirical Model for Scaling Fourier Amplitude Spectra of Strong Ground Acceleration in Terms of Modified Mercalli Intensity and Recording Site Conditions, Int. J. Earthquake Eng. and Struct. Dyn., Vol. 7, 63-71.
- Trifunac, M.D., and J.G. Anderson (1977). Preliminary Empirical Models for Scaling Absolute Acceleration Spectra, Dept. of Civil Eng., Report No. 77-03, U.S.C., Los Angeles.
- Trifunac, M.D., and J.G. Anderson (1978a). Preliminary Empirical Models for Scaling Pseudo Relative Velocity Spectra, Dept. of Civil Eng., Report No. 78-04, U.S.C., Los Angeles.
- Trifunac, M.D., and J.G. Anderson (1978b). Preliminary Empirical Models for Scaling Relative Velocity Spectra, Dept. of Civil Eng., Report No. 78-05, U.S.C., Los Angeles.

- Trifunac, M.D., and A.G. Brady (1975). On the Correlation of Seismic Intensity Scales with the Peaks of Recorded Strong Ground Motion, Bull. Seism. Soc. Amer., 65, 129-162.
- Westermo, B.D., and M.D. Trifunac (1978). Correlation of the Frequency Dependent Duration of Strong Earthquake Ground Motion with Magnitude, Epicentral Distance and the Depth of Sediments at the Recording Site, Dept. of Civil Eng., Report No. 78-12, U.S.C., Los Angeles.
- Westermo, B.D., and M.D. Trifunac (1979). Correlations of the Frequency Dependent Duration of Strong Ground Motion with the Modified Mercalli Intensity and the Depth of Sediments at the Recording Site, Dept. of Civil Eng., Report No. 79-01, U.S.C., Los Angeles.
- Wong, H.L., and M.D. Trifunac (1977). A Note on the Effects of Recording Site Conditions on Amplitudes of Strong Earthquake Ground Motion, 2-119, Sixth World Conf. Earthquake Eng., New Delhi, India.

